Article published online: 2022-08-23

Diagnostic Accuracy of Standalone T2 Dixon Sequence Compared with Conventional MRI in Sacroiliitis

R. Athira[1] Seetharaman Cannane[1] R. Thushara[1] Santhosh Poyyamoli[1] Meena Nedunchelian[1]

[1] Department of Radiology, Kovai Medical Center and Hospital, Coimbatore, Tamil Nadu, India

Indian J Radiol Imaging 2022;32:314–323.

Address for correspondence Seetharaman Cannane, DMRD, DNB, Department of Radiology, KMCH Institute of Health Science and Research, Avinashi Road, Indira Nagar, Coimbatore, Tamil Nadu 641014, India (e-mail: drcseetharaman@gmail.com).

Abstract

Aim The aim of this article was to assess the profile of T2-weighted (T2W) multipoint Dixon sequence and conventional sequences in magnetic resonance imaging (MRI) of sacroiliac joints for the diagnosis of active and chronic sacroiliitis.

Settings and Design Prospective observational study.

Materials and Methods Thirty-seven patients with sacroiliitis underwent MRI with conventional coronal oblique short tau inversion recovery, T1W sequences, and T2W multipoint Dixon sequences. T1 fat-saturated postcontrast sequences were added in active cases. Comparisons were made between conventional and T2 Dixon sequences both quantitatively and qualitatively.

Statistical Analysis Paired *t*-test was used to study the difference in contrast–noise ratio (CNR) between two groups. Chi-squared analysis with *p*-value of ≤ 0.05 was used to test the significant association of different sequences.

Results Water only images had highest mean CNR (296.35 ± 208.28) for the detection of bone marrow edema/osteitis. T1W (186.09 ± 96.96) and opposed-phase (OP) images (279.22 ± 188.40) had highest mean CNR for the detection of subchondral sclerosis and periarticular fat deposition, respectively. OP images (*p*-value <0.001) followed by fat-only (FO) images (*p*-value $= 0.001$) were superior to T1W sequences in detecting periarticular fat deposition. In-phase (IP) images in detecting subchondral sclerosis and IP and FO images in detecting cortical erosions were comparable to conventional T1W sequences (*p*-value < 0.001).

Conclusions T2 Dixon sequences are superior or comparable to conventional MR sequences in detection of sacroiliitis, except ankylosis. Hence, Dixon can be used as a single sequence to replace the multiple sequences used in conventional imaging protocol of acute sacroiliac joints due to higher image quality. It can be used as an additional sequence in case of chronic sacroiliitis to increase the confidence and accuracy of diagnosis.

Keywords
- bone marrow edema
- periarticular fat deposition
- sacroiliitis
- subchondral sclerosis
- T2 Dixon

published online
August 23, 2022

DOI https://doi.org/10.1055/s-0042-1753467.
ISSN 0971-3026.

Thieme Medical and Scientific Publishers Pvt. Ltd., A-12, 2nd Floor, Sector 2, Noida-201301 UP, India

Introduction

Sacroiliac joint is involved in multiple rheumatic and non-rheumatic disorders. Seronegative spondyloarthropathies (SpA) are the most common cause of sacroiliitis, while other causes are infection, gout, enteropathic, pyogenic, and rheumatoid arthritis.[1–4] Clinical diagnosis of sacroiliitis is difficult because patients have localized or referred pain, usually inferior to the posterior superior iliac spine, mimicking multiple other causes of back pain.[5]

Radiograph is sensitive only to chronic disease with altered joint space and subchondral bone changes. Magnetic resonance imaging (MRI) does better evaluation of joint anatomy, marrow, cartilage, subchondral bone, surrounding ligaments, and capsule and is superior in early diagnosis of acute sacroiliitis.[6,7] It is included in the new criteria defined by the Assessment of Spondylo Arthritis International Society, according to which acute sacroiliitis attributable to SpA can be visualized as bone marrow edema (BME)/osteitis, synovitis, enthesitis, or capsulitis. Presence of BME/osteitis on MRI is considered essential for diagnosis. Chronic cases are defined with subchondral sclerosis, periarticular fat deposition, articular erosions, and bony ankylosis.[8–10] MRI also helps in assessing disease activity and monitoring treatment response in cases of sacroiliitis.[2]

Conventional MRI sequences of sacroiliac joints are T1-weighted (T1W) and fat-saturated T2-weighted (T2W-FS)/STIR images. Short tau inversion recovery (STIR) hyperintensities can be confirmed with contrast-enhanced fat-saturated T1-weighted (T1W-FS-PC) images to detect osteitis.[2,10] STIR is usually sufficient for diagnosis of BME. However, in when STIR is inconclusive or to exclude possible artifacts, T1W-FS-PC sequence acts as a definitive method.[11]

Fat suppression techniques like chemical shift imaging and related Dixon-based approaches are used for detection and characterization of liver, renal, adrenal, and focal bone marrow lesions.[12] T2W multipoint Dixon technique provides four sets of post processed and automatically reconstructed images.[13,14] This Dixon sequence has a better and higher signal-to-noise ratio (SNR) in a reasonable time with homogeneous fat suppression.[13] Dixon may provide good tissue contrast without time delay compared with the conventional sequences used in detection and differentiation of sacroiliac pathologies.[12,15]

Good-quality imaging and reliable reporting play an important role in detecting the appropriate candidates with axial disease who would benefit from biologics.[16] This study evaluates the use of Dixon as a single sequence for diagnosis of sacroiliitis when compared with the conventional protocol of multiple sequences.

Method

Study Population and Study Design

This study was conducted in the Department of Radiology, Kovai Medical Center and Hospital, Coimbatore, after getting approval from the Institutional Ethics Committee and Institutional Scientific and Research Committee. Written informed consent was taken from all patients. All adult patients older than 18 years of age who had undergone MRI examination of lumbosacral spine and sacroiliac joints in our hospital during a period of August 2019 to August 2020 were included. The patients with general contraindications for MRI, patient motion during acquisition, and contraindication for MRI contrast injection were excluded from the study.

Out of the 1,325 adult patients who underwent MRI examination of lumbosacral spine and sacroiliac joints during the study period, 37 patients had evidence of sacroiliitis in conventional MRI sequences and were considered for further evaluation. A total of 63 sacroiliac joints (26 patients had bilateral involvement) were studied.

MRI Technique

MRI was done either using a Siemens MAGNETOM Skyra 3T MRI or Philips Ingenia 1.5T MRI with dedicated phased array coils (►**Table 1**). Thirty-two patients underwent scans in 1.5 T system and 5 patients in 3T system. The acquired sequences in the routine protocol were coronal oblique STIR sequences and T1W turbo spin echo sequences. A T2W multipoint Dixon sequence in coronal oblique plane was added to the protocol. After the administration of gadolinium, T1W-FS-PC sequence was performed in the coronal oblique plane if hyperintense signal was noted in IR sequence.

Reference for normal bone marrow signal was taken as the sacral interforaminal bone marrow signal. Affected bone marrow areas are typically periarticular. For all sequences, filed of view was 220 mm.

Image Analysis

Qualitative Analysis

Active inflammation of SI joint was diagnosed if BME was seen in STIR images and osteitis seen in T1W-FS-PC images. Chronic inflammation was diagnosed if subchondral sclerosis, periarticular fat deposition, ankylosis, and articular erosions were seen in T1W sequences. In T2W multipoint Dixon sequence images, active inflammation was looked for in water-only images and chronic inflammation in in-phase (IP), opposed-phase (OP), and fat-only (FO) images.

Quantitative Analyses

For all patients, contrast–noise ratios (CNRs) of active subchondral bone marrow lesions, subchondral sclerosis, and periarticular fat deposition were calculated using:

CNR = [Mean *L*– Mean *BM*] / SD *air*,

Mean *L*: mean signal intensity of the largest lesion in one sacroiliac joint,
Mean *BM*: mean signal intensity of the normal-appearing bone marrow near the lesion,
SD *air*: Standard deviation (SD) of the signal intensity of the airspace free of artifact and close to the site of previously obtained signal-intensity measurements.[2]

For the same active lesions, CNR was calculated on STIR images, T1W-FS-PC images, and water-only T2W multipoint

Table 1 MRI parameters in 1.5T and 3T scanner systems

	Scanner	STIR	T1W	T1W-FS-PC	T2-Dixon
TR (ms)	1.5 T	2500–4000	400–600	400–750	3000–5000
	3 T	370	700	574	4230
TE (ms)	1.5T	55	8	8	80
	3 T	36	9	9	81
Turbo factor	1.5 T	16	5	5	18
	3 T	16	5	5	15
Slice thickness (mm)	1.5 T	3.5	3.5	3.5	3.5
	3 T	3	3	3	3
Intersection gap (mm)	1.5 T	0.35	0.35	0.35	0.35
	3 T	0.3	0.3	0.3	0.3

Abbreviations: MRI, magnetic resonance imaging; STIR, short tau inversion recovery; T1W-FS-PC, contrast-enhanced fat-saturated T1-weighted; TR, repetition time; TE, time to echo.

Dixon images. For the same chronic lesions, CNR was calculated on T1W images, IP, OP, and FO T2W multipoint Dixon images. The largest lesion in each sacroiliac joint of each patient was evaluated. A same-sized round region of interest was used in all sequences for measuring signal intensity.

Statistical Analysis

Statistical Package for Social Sciences (SPSS) version 20 was employed to analyze data. Continuous data was analyzed for its mean, median, and SD. Categorical variable was analyzed using chi-squared test and "*p*" value of ≤ 0.05 was considered as statistically significant. Data was presented as mean $\pm$ SD for continuous variables and as percentages for categorical variables. The mean and SD of the CNR value for each prognostic factor were calculated. The analysis was done to test if there is any statistically significant difference in CNR values between groups. Paired *t*-test for independent sample was used to study the difference in CNR between two groups. Chi-squared analysis was used to test the significant association in qualitative analysis of different sequences.

Results

A total of 37 patients (20 males and 17 females) and 63 joints (26 patients had bilateral, 7 had right, and 4 had left-sided joint involvement) were studied. The age of the patients ranged from 19 to 75 years (mean: 38.1 $\pm$ 11.8 years). Among these 63 cases of sacroiliitis, 14 (22.2%) were in acute stage, 29 (46.1%) were in chronic stage, and 20 cases (31.7%) were in acute on chronic stage. So, a total of 34 SI joints in acute stage and 49 SI joints in chronic stage were evaluated. Qualitative analysis was done with visual assessment and quantitative analysis was done with CNR of the largest lesion in each joint.

Qualitative Analysis

Acute Sacroiliitis

The signal changes consistent with BME/osteitis were visually assessed with STIR, T1W-FS-PC images, and WO image set of Dixon sequence (►**Fig. 1A–C** and ►**Fig. 2A–C**) and graded as mild and moderate signal changes. All signal changes noted in STIR and T1W-FS-PC images were also noted in WO images, suggestive of 100% agreement. The chi-squared test to assess the association between WO and STIR image sets and WO and T1W-FS-PC image sets yielded a *p*-value of < 0.001, suggestive of significant strong association between the image sets in both the groups.

Chronic Sacroiliitis

The signal changes of bone marrow consistent with subchondral sclerosis, periarticular fat deposition, articular erosions, and ankylosis were visually assessed with T1W images, IP, OP, and FO T2W multipoint Dixon images and graded as mild, moderate, and severe changes. All cases detected in T1W images were noted in IP and FO images, suggestive of 100% agreement. No new cases were diagnosed with Dixon sequences.

A total of 44 cases in T1W, IP, and FO images and 38 cases in OP images demonstrated subchondral sclerosis (►**Fig. 3A–D**). On assessing the association of the above three image sets of Dixon sequence with T1W images, the IP image sets showed a *p*-value <0.001, suggestive of strong association. The FO and OP images showed no statistically significant association with T1W images in detection of subchondral sclerosis.

A total of 41cases demonstrated subchondral fat deposition in T1W, IP, OP, and FO images (►**Fig. 4A–D**). On assessing the association of the above three image sets of Dixon sequence with T1W images, all the three image sets showed a *p*-value of <0.001, suggestive of strong association.

A total of six cases demonstrated ankylosis in T1W, IP, OP, and FO images (►**Fig. 5A–D**). On assessing the association of the above three image sets of Dixon sequence with T1W images, all the three image sets showed a *p*-value of > 0.05, suggestive of no association.

A total of 44 cases demonstrated cortical erosions in T1W, IP, and FO images and 24 cases in OP images (►**Fig. 6A–D**). On assessing the association of the above three image sets of

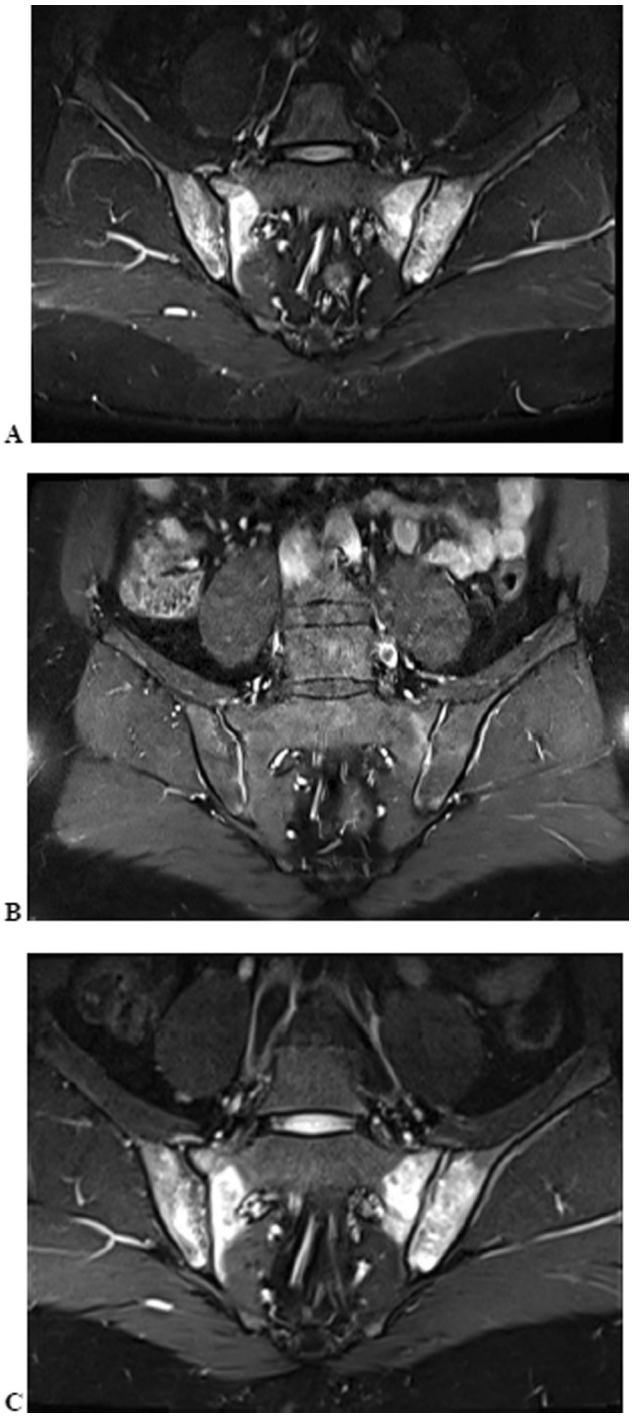

Fig. 1 Oblique coronal sections of short tau inversion recovery (**A**), fat-saturated T1 postcontrast (**B**), and water only images (**C**) of bone marrow edema/osteitis in a case of bilateral acute sacroiliitis.

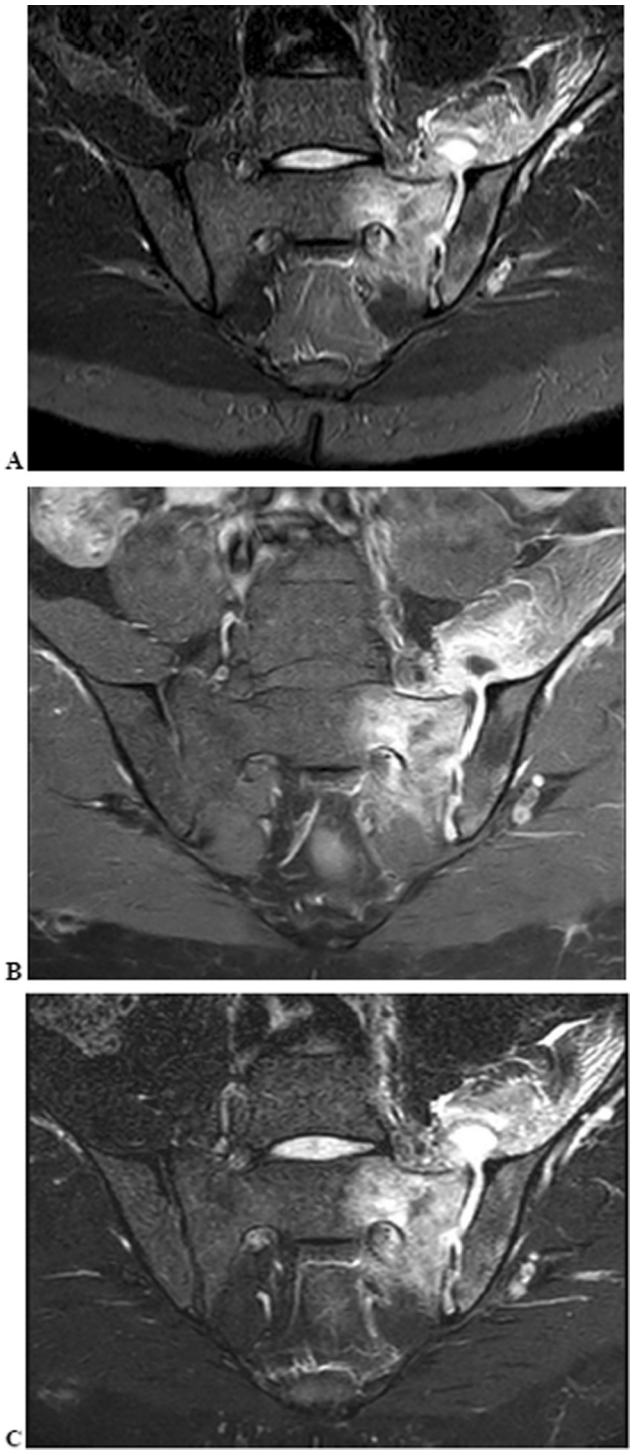

Fig. 2 Oblique coronal sections of short tau inversion recovery (**A**), fat-saturated T1 postcontrast (**B**), and water only images (**C**) of a case of acute infective left sacroiliitis showing collection and bone marrow edema/osteitis.

Dixon sequence with T1W images, IP and FO sets showed a *p*-value <0.001, suggestive of significant strong association.

Quantitative Analysis

Acute Sacroiliitis

On evaluating 34 cases of acute sacroiliitis quantitatively, the mean CNR of largest lesions was highest for WO images (296.35; SD: 208.28) compared with STIR and T1W-FS-PC sequences (►**Fig. 7**). On applying paired *t*-test, statistically significant difference was noted between WO and STIR image sets (p-value < 0.001) and between WO and T1W-FS-PC image sets (p-value $= 0.002$) (►**Table 2**).

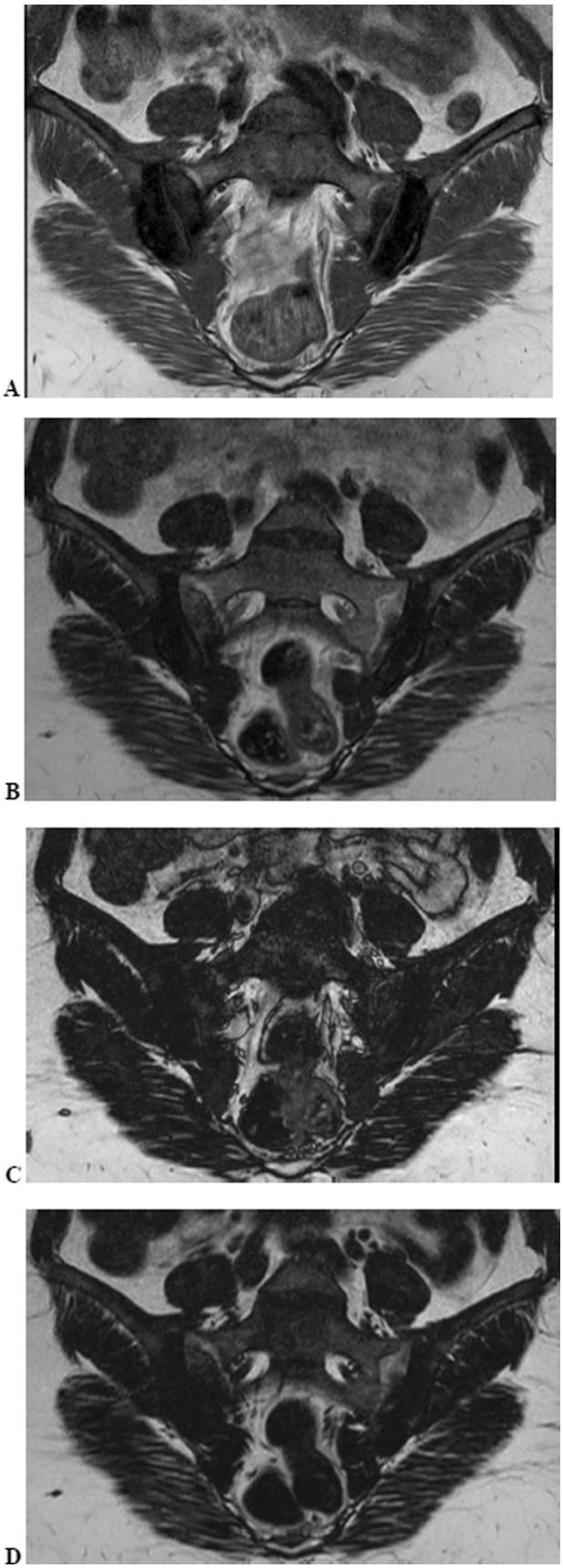

Fig. 3 Oblique coronal sections of T1-weighted (**A**), in-phase (**B**), opposed-phase (**C**), and fat only images (**D**) of subchondral sclerosis in bilateral chronic sacroiliitis.

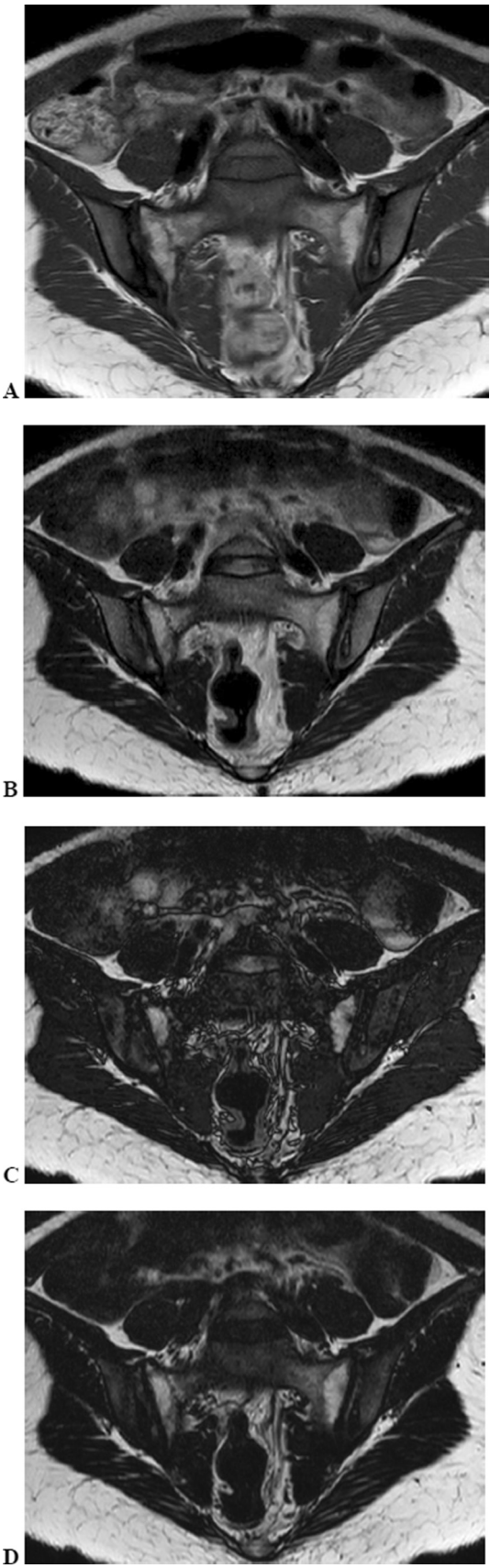

Fig. 4 Oblique coronal sections of T1-weighted (**A**), in-phase (**B**), opposed-phase (**C**), and fat only images (**D**) of periarticular fat deposition in bilateral chronic sacroiliitis.

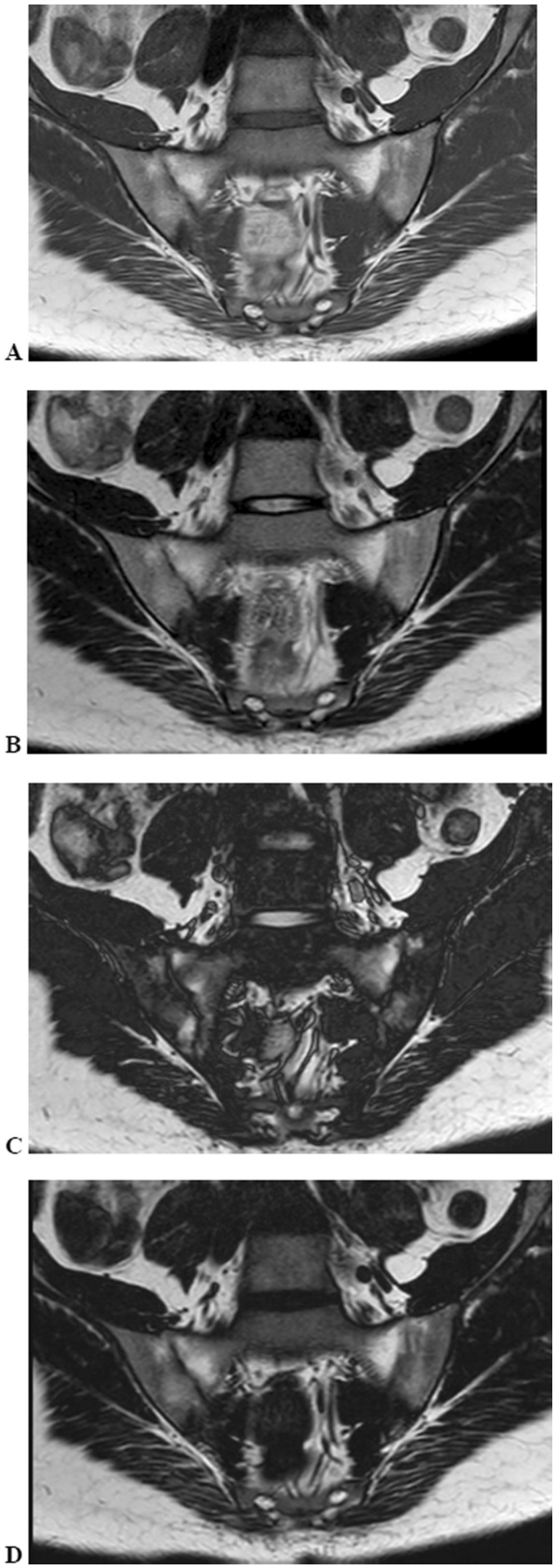

Fig. 5 Oblique coronal sections of T1-weighted (**A**), in-phase (**B**), opposed-phase (**C**), and fat only images (**D**) of ankylosis in bilateral chronic sacroiliitis.

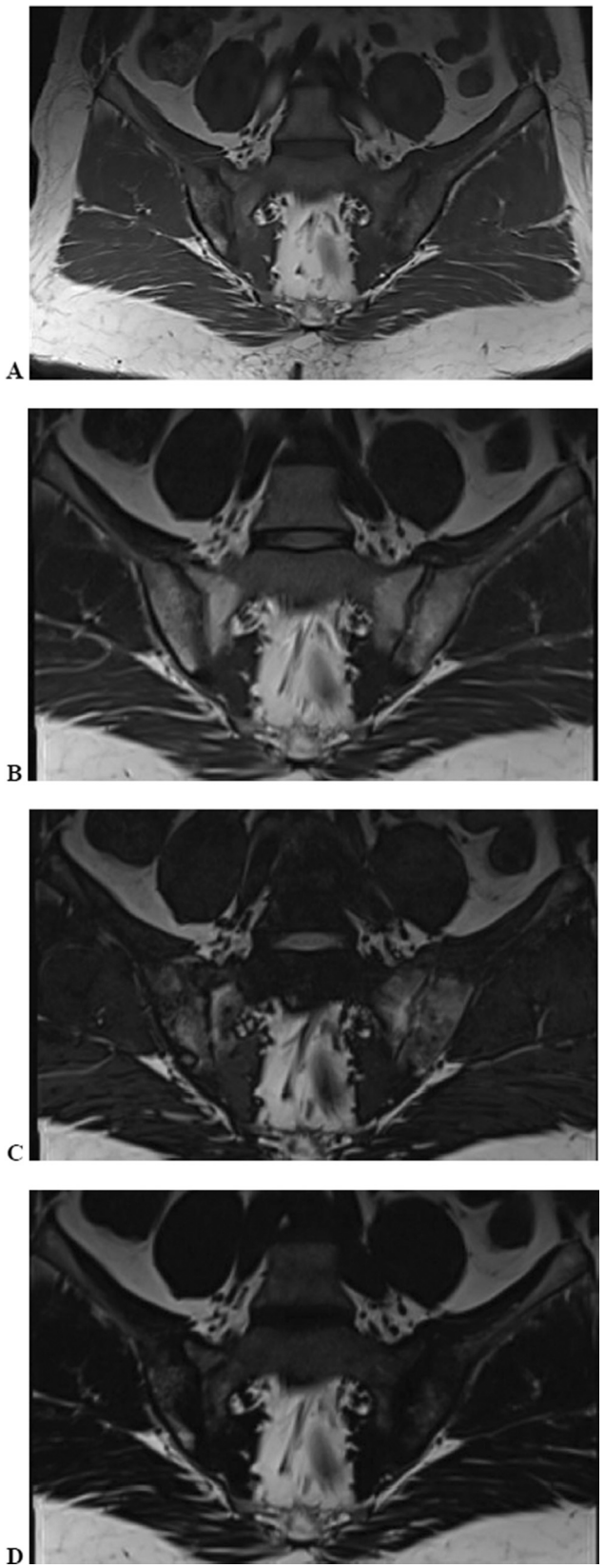

Fig. 6 Oblique coronal sections of T1-weighted (**A**), in-phase (**B**), opposed-phase (**C**), and fat only images (**D**) of erosions in bilateral chronic sacroiliitis.

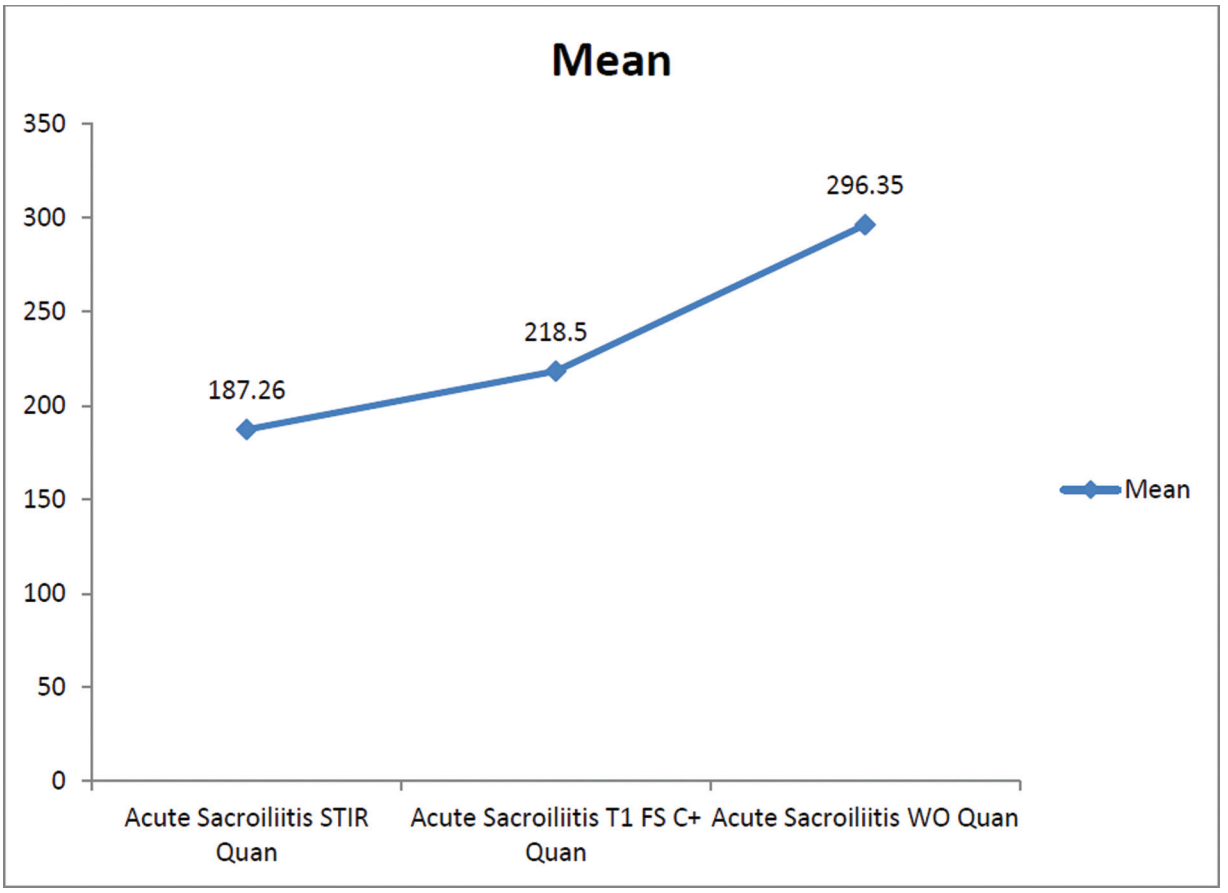

Fig. 7 Distribution of mean values of contrast–noise ratio of bone marrow edema/osteitis in acute cases. STIR, short tau inversion recovery.

Chronic Sacroiliitis

Subchondral Sclerosis

On evaluating 44 cases of chronic sacroiliitis with subchondral sclerosis quantitatively, the mean CNR of largest lesions was highest for T1W images (186.09; SD: 96.96) compared with IP, OP, and FO sets of T2 Dixon sequences (►**Table 3**). On applying paired *t*-test, statistically significant difference was noted between T1W and OP image set and T1W and FO image sets (p-value < 0.001). A p-value was not statistically significant (>0.05) when T1W image was compared with IP images.

Fat Deposition

On evaluating 41 cases of chronic sacroiliitis with fat deposition quantitatively, the mean CNR of largest lesions was highest for OP images (279.22; SD: 188.40) compared with T1W, IP, and FO images (►**Table 4**). On applying paired *t*-test, statistically significant difference was noted between T1W and OP image set (p-value: < 0.001) and T1W and FO image set (p-value $= 0.001$). A p-value was not statistically significant (p-value: > 0.05) when T1W image was compared with IP images.

Table 2 Statistical analysis of CNR of BME/osteitis in acute sacroiliitis

Acute sacroiliitis	Mean	SD	*p*-Value
STIR	187.26	108.31	< 0.001
WO	296.35	208.28	
T1W-FS-PC	218.50	145.59	0.002
WO	296.35	208.28	

Abbreviations: BME, bone marrow edema; CNR, contrast–noise ratio; SD, standard deviation; STIR, short tau inversion recovery; T1W-FS-PC, contrast-enhanced fat-saturated T1-weighted.

Table 3 Statistical analysis of CNR of subchondral sclerosis in chronic sacroiliitis

Subchondral sclerosis	Mean	SD	*p*-Value
T1W	186.09	96.96	0.107
IP	162.32	109.22	
T1W	189.50	89.65	< 0.001
OP	50.73	34.36	
T1W	186.09	96.96	< 0.001
FO	122.27	63.48	

Abbreviations: CNR, contrast–noise ratio; FO, fat only; IP, in-phase; OP, opposed-phase; SD, standard deviation; T1W, T1-weighted.

Table 4 Statistical analysis of CNR of fat deposition in chronic sacroiliitis

Fat deposition	Mean	SD	*p*-Value
T1W	153.41	101.61	0.338
IP	141.71	121.42	
T1W	153.41	101.61	< 0.001
OP	279.22	188.40	
T1W	153.41	101.61	0.001
FO	193.44	95.96	

Abbreviations: CNR, contrast–noise ratio; FO, fat only; IP, in-phase; OP, opposed-phase; SD, standard deviation; T1W, T1-weighted.

On comparing the scan times in 3T Siemens MRI, collective scan time for routine STIR (53 seconds), T1W imaging (1 minute, 41seconds), and T1W-FS-PC image (1 minute, 5 seconds) is 3 minutes, 39 seconds. The time for T2 multipoint Dixon sequence is 2 minutes, 37 seconds.

In 1.5T Philips MRI, collective scan time for routine STIR (1 minute, 45 seconds), T1W imaging (2 minutes, 19 seconds), and T1W-FS-PC (3 minutes, 34 seconds) imaging is 7 minutes, 38 seconds. The time for T2 multipoint Dixon sequence is 3 minutes, 35 seconds.

Discussion

The use of Dixon sequences in various clinical settings has shown to provide a better fat suppression and image quality when compared with the conventional methods. On the basis of this rationale, Dixon sequence is expected to be equal or superior to the conventional imaging of sacroiliac joint. This could reduce the scanning time by decreasing a multisequence protocol to a single Dixon T2W sequence. It is also expected to improve the image quality leading to increased diagnostic confidence. The aim of the study was to assess the profile of T2W multipoint Dixon sequence and conventional sequences in MRI of sacroiliac joints for the diagnosis of active and chronic sacroiliitis.

Only very few studies have been conducted regarding the role of Dixon in the evaluation of sacroiliac joint. The study conducted by Özgen in 2017 concluded that T2W multipoint Dixon sequence was superior to conventional MRI sequences in depicting diagnostic signs of active and chronic sacroiliitis and therefore may be used as a single sequence.[2]

In our study, the bone marrow lesions in acute sacroiliitis were equally appreciated in STIR, T1W-FS-PC, and WO images. The WO images were superior to STIR and T1W-FS-PC images quantitatively for the detection of BME/osteitis. However, the administration of contrast did not add to the diagnosis of any new cases of sacroiliitis.

In chronic sacroiliitis, subchondral sclerosis was demonstrated adequately in IP sequences and was comparable with T1W sequences. The diagnosis of subchondral sclerosis was difficult in FO and OP sequences. No statistically significant difference was noted between T1W and IP images on quantitative analysis though mean CNR was higher for T1W images. T1W sequence was superior to FO and OP sequences and was comparable to IP sequences.

Periarticular fat deposition was demonstrated in all the three Dixon sequences. The signal changes in OP images were qualitatively comparable to or better than the T1W sequences. The OP images followed by FO images were superior in the assessment of periarticular fat deposition compared with routine sequences.

In assessing ankylosis qualitatively, no statistically significant association existed between T1W sequence and any of the imaging sets of Dixon sequence. Concerning cortical erosions, all lesions noted in the conventional T1W images were redemonstrated in IP image sets. Also, the lesions in IP and FO image sets were comparable to T1W images. However, the diagnosis of these conditions was difficult in OP images.

Therefore, in our study, using T2W multipoint Dixon sequence for analysis of sacroiliitis, WO images were superior to the conventional imaging modality in detecting acute bone marrow lesions; IP images were comparable to conventional T1W sequences in detecting subchondral sclerosis and OP images followed by FO images were superior to T1W images in detecting periarticular fat deposition. Detection of cortical erosions by IP and FO image sets were comparable to T1W images. Diagnosis of ankylosis was difficult with the Dixon sequences.

According to the study conducted by Özgen in 2017, who studied 34 lesions among 73 patients, a similar outcome was obtained. However, the T2W-FS sequence was considered superior to postcontrast images in acute stage. He showed that use of IP images could result in a statistically significant difference in detecting subchondral sclerosis. T1W images had the minimum CNR considering periarticular fat deposition and statistically significant difference was noted between T1W and OP images only.[2]

The advantage of Dixon is that due to their insensitivity to local magnetic field inhomogeneities, it provides homogenous fat suppression compared with other fat saturation techniques. These techniques can also be used for fat quantification. Dixon techniques can be implemented in both gradient echo and spin-echo sequences, with some technical adaptation.[13] However, metallic artifacts due to larger prosthesis result in low-quality images in case of Dixon technique. In this setting, STIR remains the preferred technique.[12,13] However, it has a low SNR compared with Dixon sequences and cannot be used as a postcontrast sequence. Hence, Dixon is a preferred in knee with small metallic material, in ankle or for spinal arthrodesis due to its higher SNR. It is also used when fat suppression is needed in postcontrast images as in inflammatory/infectious changes in the proximity of metallic implants.[13]

Dixon sequence is widely used in many fields in recent history. The Dixon sequences provide both better image quality and increased CNR when compared with the routine fat suppression sequences used.[17] Due to the improved CNR and decreased acquisition time with advantage that it can be used in both T1W and T2W sequences, it is considered equal to or superior to different conventional modalities and in

imaging of neck, breast, abdomen, and female pelvic conditions.[13,17–21] It is also studied in recent fields of renal dynamic contrast-enhanced MRI and cardiac imaging.[22,23] Dixon sequence has many applications in musculoskeletal imaging where the bone marrow replacement lesions and fractures can be detected with increased accuracy.[12,24–26]

Most of these studies suggest that Dixon as a single sequence can replace the standard combination protocol of morphologic sequences followed in these areas.

Conclusion

In detecting acute sacroiliitis, WO images of the T2 multipoint Dixon sequence are superior to the conventional MRI sequences. Thus, Dixon can be used as a single sequence to replace the multiple sequences used in conventional imaging protocol of sacroiliac joints due to higher image quality and reduced scan time in case of acute sacroiliitis.

In detecting chronic sacroiliitis, OP images followed by FO images are superior to T1W images in detecting periarticular fat deposition and IP images are comparable to T1W sequences in detecting subchondral sclerosis. Detection of cortical erosions by IP and FO image sets is comparable to T1W images. Diagnosis of ankylosis is difficult with the Dixon sequences. Hence, Dixon can be used as an additional sequence to the existing standard sequences in case of chronic sacroiliitis, especially to increase the confidence of the radiologist and accuracy in diagnosis.

Limitations

Since the sample size is small, larger studies are needed for better analysis of the possibilities of Dixon sequences. The data involves scans done in both 1.5T and 3T MRIs from different vendors. The diagnosis of ankylosis with Dixon technique showed no significant association with the conventional sequence, likely due to limited number of patients studied with ankylosis. Both the conventional and Dixon sequences were analyzed only by one observer and was done at the same time, which may cause bias affecting the outcome. Sacroiliitis due to multiple causes like inflammatory and infective etiologies is included in the study group. The reference for diagnosis of sacroiliitis was taken as the conventional imaging protocol and was not proved by laboratory findings or follow-ups. Follow-up of the cases with Dixon sequence is not done to evaluate the serial change in signal characters, and thereby its scope in assessing treatment response is suboptimally assessed.

Recommendations

Dedicated studies with higher patient population are needed to support the use of Dixon sequence as the primary sequence for screening sacroiliac joints. Also, more patients with ankylosis need to be studied to assess the role of Dixon sequence in its diagnosis. Proper administration of matching and blinding techniques is needed in the future studies to avoid errors and bias. Role of Dixon technique in follow-up cases also needs to be studied in detail.

Sources of Support
Nil.

Conflict of Interest
None.

Acknowledgment
Nil.

References

1 Alqatari S, Visevic R, Marshall N, Ryan J, Murphy G. An unexpected cause of sacroiliitis in a patient with gout and chronic psoriasis with inflammatory arthritis: a case report. BMC Musculoskelet Disord 2018;19(01):126
2 Özgen A. The value of the T2-weighted multipoint Dixon sequence in MRI of sacroiliac joints for the diagnosis of active and chronic sacroiliitis. AJR Am J Roentgenol 2017;208(03):603–608
3 Murphey MD, Wetzel LH, Bramble JM, Levine E, Simpson KM, Lindsley HB. Sacroiliitis: MR imaging findings. Radiology 1991; 180(01):239–244
4 Slobodin G, Hussein H, Rosner I, Eshed I. Sacroiliitis - early diagnosis is key. J Inflamm Res 2018;11:339–344
5 Tilvawala K, Kothari K, Patel R. Sacroiliac joint: a review. Indian J Pain. 2018;32(01):4
6 Puhakka KB, Melsen F, Jurik AG, Boel LW, Vesterby A, Egund N. MR imaging of the normal sacroiliac joint with correlation to histology. Skeletal Radiol 2004;33(01):15–28
7 Montandon C, Costa MAB, Carvalho TN, Montandon Júnior ME, Teixeira K-I-SS. Sacroiliíte: avaliação por imagem. Radiol Bras 2007;40(01):53–60
8 Kang Y, Hong SH, Kim JY, et al. Unilateral sacroiliitis: differential diagnosis between infectious sacroiliitis and spondyloarthritis based on MRI findings. AJR Am J Roentgenol 2015;205(05): 1048–1055
9 Prakash D, Prabhu SM, Irodi A. Seronegative spondyloarthropathy-related sacroiliitis: CT, MRI features and differentials. Indian J Radiol Imaging 2014;24(03):271–278
10 Rudwaleit M, Jurik A-G, Hermann KG, et al. Defining activesacroiliitis on magnetic resonance imaging (MRI) for classification of axial spondyloarthritis: a consensual approach by the ASAS/OMERACT MRI group. Ann Rheum Dis 2009;68(10):1520–1527
11 Hermann K-G, Bollow M. Magnetic resonance imaging of sacroiliitis in patients with spondyloarthritis: correlation with anatomy and histology. Röfo Fortschr Geb Röntgenstr Nuklearmed 2014; 186(03):230–237
12 Pezeshk P, Alian A, Chhabra A. Role of chemical shift and Dixon based techniques in musculoskeletal MR imaging. Eur J Radiol 2017;94:93–100
13 Guerini H, Omoumi P, Guichoux F, et al. Fat suppression with Dixon techniques in musculoskeletal magnetic resonance imaging: a pictorial review. Semin Musculoskelet Radiol 2015;19(04):335–347
14 Ma J. Dixon techniques for water and fat imaging. J Magn Reson Imaging 2008;28(03):543–558
15 Tsoi C, Griffith JF, Lee RKL, Wong PCH, Tam LS. Imaging of sacroiliitis: current status, limitations and pitfalls. Quant Imaging Med Surg 2019;9(02):318–335
16 Orr KE, Andronikou S, Bramham MJ, Holjar-Erlic I, Menegotto F, Ramanan AV. Magnetic resonance imaging of sacroiliitis in children: frequency of findings and interobserver reliability. Pediatr Radiol 2018;48(11):1621–1628
17 Takatsu Y, Akasaka T, Miyati T. The Dixon technique and the frequency-selective fat suppression technique in three-

dimensional T1 weighted MRI of the liver: a comparison of contrast-to-noise ratios of hepatocellular carcinomas-to-liver. Br J Radiol 2015;88(1050):20150117
18 Kalovidouri A, Firmenich N, Delattre BMA, et al. Fat suppression techniques for breast MRI: Dixon versus spectral fat saturation for 3D T1-weighted at 3 T. Radiol Med (Torino) 2017;122(10): 731–742
19 Gaddikeri S, Mossa-Basha M, Andre JB, Hippe DS, Anzai Y. Optimal fat suppression in head and neck MRI: comparison of multipoint Dixon with 2 different fat-suppression techniques, spectral presaturation and inversion recovery, and STIR. AJNR Am J Neuroradiol 2018;39(02):362–368
20 Ding Y, Rao SX, Chen CZ, Li RC, Zeng MS. Usefulness of two-point Dixon fat-water separation technique in gadoxetic acid-enhanced liver magnetic resonance imaging. World J Gastroenterol 2015;21 (16):5017–5022
21 Beddy P, Rangarajan RD, Kataoka M, Moyle P, Graves MJ, Sala E. T1-weighted fat-suppressed imaging of the pelvis with a dual-echo Dixon technique: initial clinical experience. Radiology 2011;258 (02):583–589
22 Farrelly C, Shah S, Davarpanah A, Keeling AN, Carr JC. ECG-gated multiecho Dixon fat-water separation in cardiac MRI: advantages over conventional fat-saturated imaging. AJR Am J Roentgenol 2012;199(01):W74-83
23 de Boer A, Leiner T, Vink EE, Blankestijn PJ, van den Berg CAT. Modified Dixon-based renal dynamic contrast-enhanced MRI facilitates automated registration and perfusion analysis. Magn Reson Med 2018;80(01):66–76
24 Maeder Y, Dunet V, Richard R, Becce F, Omoumi P. Bone marrow metastases: T2-weighted Dixon spin-echo fat images can replace T1-weighted spin-echo images. Radiology 2018;286(03):948–959
25 Yoo HJ, Hong SH, Kim DH, et al. Measurement of fat content in vertebral marrow using a modified Dixon sequence to differentiate benign from malignant processes. J Magn Reson Imaging 2017; 45(05):1534–1544
26 Kim YP, Kannengiesser S, Paek M-Y, et al. Differentiation between focal malignant marrow-replacing lesions and benign red marrow deposition of the spine with T2*-corrected fat-signal fraction map using a three-echo volume interpolated breath-hold gradient echo Dixon sequence. Korean J Radiol 2014;15(06):781–791

